

Propagation of plane wave in transversely isotropic magneto-thermoelastic material with multi-dual-phase lag and two temperature

Parveen Lata^{1a}, Iqbal Kaur^{*1} and Kulvinder Singh²

¹Department of Basic and Applied Sciences, Punjabi University, Patiala, Punjab, India

²Kurukshetra University Kurukshetra, Haryana, India

(Received April 5, 2020, Revised May 24, 2020, Accepted May 25, 2020)

Abstract. This research is devoted to the study of plane wave propagation in homogeneous transversely isotropic (HTI) magneto-thermoelastic rotating medium with combined effect of Hall current and two temperature due to multi-dual-phase lag heat transfer. It is analysed that, for 2-D assumed model, three types of coupled longitudinal waves (quasi-longitudinal, quasi-transverse and quasi-thermal) are present. The wave characteristics like phase velocity, specific loss, attenuation coefficients, energy ratios, penetration depths and amplitude ratios of transmitted and reflected waves are computed numerically and illustrated graphically and compared for different theories of thermoelasticity. Some particular cases are also derived from this research.

Keywords: transversely isotropic; magneto-thermoelastic; rotation; multi-dual-phase lag heat transfer; hall current; two temperature; plane wave propagation

1. Introduction

The application of thermal shock and the magnetic field, produces an induced magnetic and electric field as well as deformation in the media. These magnetic and electric field produce the voltage (known as Hall voltage) across conductor. The composite material such as a magneto-thermoelastic material is gaining considerable importance since the last decade as these materials shows the coupling effect between the magnetic and electric fields. Study of plane wave propagation in a magneto-thermoelastic solids is significant because of its applications in the area of inspecting materials, magnetometers, geophysics, nuclear fields and related topics. So significant attention is given in the area of plane wave propagation in thermoelastic and magneto-thermoelastic (MT) medium.

Borejko (1996) considered the coefficients of transmission and reflection for 3D plane waves in elastic media. Sinha and Elsibai (1997) discussed the refraction and reflection of thermoelastic waves with two relaxation times at the boundary of two semi-infinite media. Ting (2004) explored

*Corresponding author, Ph.D. Scholar, E-mail: bawahanda@gmail.com

^aAssociate Professor, E-mail: parveenlata@pbi.ac.in

^bAssistant Professor, E-mail: ksingh2015@kuk.ac.in

propagation of surface wave in an anisotropic rotating media. Othman and Song (2006; 2008) presented different hypotheses about magnetothermoelastic waves in homogeneous isotropic medium. Kumar and Chawla (2011) discussed the plane wave propagation in anisotropic two and three phase lag (TPL) model. Deswal and Kalkal (2015) discussed the problem in a surface suffering a time dependent thermal shock for thermo-viscoelastic interactions in a 3-D homogeneous isotropic media.

The reflection of plane periodic wave in thermoelastic micropolar homogeneous transversely isotropic (HTI) media had been studied by Kumar and Gupta (2012) to find out the complex velocities of the four waves i.e., quasi-longitudinal displacement (qLD), quasi-transverse microrotational (qTM), quasi-transverse displacement (qTD) and quasi thermal (qT) waves. Abouelregal (2013) has investigated the induced displacement, temperature, and stress fields in transversely isotropic boundless medium with cylindrical cavity with moving and harmonically heat source with dual phase lag (DPL) model. The effects of reflection and refraction are studied by Gupta (2015) at the boundary of elastic and a thermoelastic diffusion media, for plane waves by expanding the Fick law with DPL diffusion model with delay times of both mass flow as well as potential gradient. Beside, Kumar *et al.* (2016) depicted the effect of time, thermal and diffusion phase lags for an axisymmetric heat supply in a ring for DPL model for transfer of heat and diffusion by considering upper and lower surfaces of the ring as friction free.

Youssef (2013, 2016) proposed a two-temperature model for an elastic half-space with constant elastic parameters and with generalized thermoelasticity without energy dissipation. Sharma and Kaur (2015) had investigated the transverse vibrations due to time varying patch loads in homogeneous thermoelastic thin beams. However, Kumar *et al.* (2016) had explored the uncertainties due to thermomechanical sources (concentrated and distributed) using Laplace and Fourier transform technique in a homogeneous transversely isotropic thermoelastic (HTIT) rotating medium with magnetic effect, two temperature and by G-N theory with and without energy dissipation w.r.t. thermomechanical sources. Kumar *et al.* (2017) investigated the Rayleigh waves in a MT rotating media in the presence of hall current and two temperature.

Othman *et al.* (2017) proposed a model for generalized magneto-thermoelasticity in an isotropic elastic medium rotating with a uniform angular velocity and with two-temperature and initial stress under LS (Lord-Shulman), GL (Green-Lindsay) and CT (coupled theory) theories of generalized thermoelasticity. Kumar and Kansal (2017) studied the reflected and refracted waves in MT diffusive half-space with voids. Maitya *et al.* (2017) presented plane wave propagation in fibre-reinforced medium with GN -I and II type of thermoelasticity theories and rotation.

Alesemi (2018) demonstrated the efficiency of the thermal relaxation time depending upon LS theory, Coriolis and Centrifugal Forces on plane wave's reflection coefficients in an anisotropic MT rotating medium. Despite of this several researchers worked on different theory of thermoelasticity Marin (1996, 2009, 2010), Lee *et al.* (2002), Craciun and Soós (2006), Craciun *et al.* (2008), Ezzat *et al.* (2016), Marin *et al.* (2016), Ezzat *et al.* (2012), Ezzat *et al.* (2015), Hassan *et al.* (2018), Marin and Nicaise (2016), Ezzat and El-Bary (2017), Othman and Marin (2017), Chauthale *et al.* (2017), Kumar *et al.* (2018), Marin *et al.* (2017), Bhatti *et al.* (2019a, 2019b), Lata and Kaur (2019a, 2019b, 2019c), Lata and Kaur (2019d, 2019e), Bhatti *et al.* (2020a, 2020b) and Zhang *et al.* (2020). Despite of these, not much work has been carried out in study of the plane wave propagation with combined effect of hall current, multi-dual phase lag theory of heat transfer and two temperature.

In this paper, we have attempted to study the plane wave propagation with combined effect of hall current, multi-phase lag heat transfer and two temperature in HTI magneto thermoelastic rotating medium.

2. Basic equations

Following Kumar *et al.* (2016), the simplified Maxwell's equations for a slowly moving and conducting elastic solid are

$$\nabla \times \mathbf{h} = \mathbf{J} + \epsilon_0 \dot{\mathbf{E}}, \tag{1}$$

$$\nabla \times \mathbf{E} = -\mu_0 \dot{\mathbf{h}}, \tag{2}$$

$$\mathbf{E} = -\mu_0(\dot{\mathbf{u}} + \mathbf{H}_0), \tag{3}$$

$$\nabla \cdot \mathbf{h} = 0. \tag{4}$$

And generalized Ohm's law for finite conductivity and hall current effect is

$$\mathbf{J} = \frac{\sigma_0}{1 + m^2} \left(\mathbf{E} + \mu_0 \left(\dot{\mathbf{u}} \times \mathbf{H} - \frac{1}{en_e} \mathbf{J} \times \mathbf{H}_0 \right) \right). \tag{5}$$

Maxwell stress components are given by

$$T_{ij} = \mu_0(H_i h_j + H_j h_i - H_k h_k \delta_{ij}). \tag{6}$$

The constitutive relation for an anisotropic thermoelastic medium is given by

$$t_{ij} = c_{ijkl} e_{kl} - \beta_{ij} T. \tag{7}$$

Here c_{ijkl} ($c_{ijkl} = c_{klij} = c_{jikl} = c_{ijlk}$) are elastic parameters and having symmetry ($c_{ijkl} = c_{klij} = c_{jikl} = c_{ijlk}$). The basis of these symmetries of c_{ijkl} is due to

- i. The stress tensor is symmetric, which is only possible if ($c_{ijkl} = c_{jikl}$)
- ii. If a strain energy density exists for the material, the elastic stiffness tensor must satisfy $c_{ijkl} = c_{klij}$
- iii. From stress tensor and elastic stiffness tensor symmetries infer ($c_{ijkl} = c_{ijlk}$) and $c_{ijkl} = c_{jikl} = c_{ijlk}$

Equation of motion as described by Lata and Kaur (2018) for an anisotropic magneto-thermoelastic medium rotating uniformly with angular velocity Ω is given by

$$t_{ij,j} + F_i = \rho \{ \ddot{\mathbf{u}}_i + (\Omega \times (\Omega \times \mathbf{u}))_i + (2\Omega \times \dot{\mathbf{u}})_i \}, \tag{8}$$

where $F_i = \mu_0(\mathbf{J} \times \mathbf{H}_0)_i$ are the components of Lorentz force. The terms $\Omega \times (\Omega \times \mathbf{u})$ and $2\Omega \times \dot{\mathbf{u}}$ are the centripetal acceleration and Coriolis acceleration due to the time-varying motion respectively. A comma followed by suffix denotes spatial derivative and a superposed dot denotes derivative with respect to time.

Following Zenkour *et al.* (2018) heat conduction equation with multi-dual-phase lag heat transfer is

$$K_{ij} \mathcal{L}_\theta \varphi_{,ij} = \mathcal{L}_q \frac{\partial}{\partial t} (\beta_{ij} T_0 u_{i,j} + \rho C_E T), \tag{9}$$

Where

$$\mathcal{L}_\theta = 1 + \sum_{r=1}^{R_1} \frac{\tau_\theta^r}{r!} \frac{\partial^r}{\partial t^r}, \quad \text{and} \quad \mathcal{L}_q = q + \tau_0 \frac{\partial}{\partial t} + \sum_{r=2}^{R_2} \frac{\tau_q^r}{r!} \frac{\partial^r}{\partial t^r}.$$

$$\begin{aligned}
\beta_{ij} &= c_{ijkl}\alpha_{ij} \\
e_{ij} &= \frac{1}{2}(u_{i,j} + u_{j,i}), \quad i, j = 1, 2, 3. \\
T &= \varphi - a_{ij}\varphi_{,ij} \\
T &= \varphi - a_{ij}\varphi_{,ij}
\end{aligned} \tag{10}$$

Where, $0 \leq \tau_\theta < \tau_q$. Generally, the value of $R_1 = R_2 = R$ may reach 5 or more according to refined multi-dual-phase-lag theory required while ϱ is 0 or 1 according to the thermoelasticity theory.

3. Formulation and solution of the problem

We consider a perfectly conducting HTI magneto-thermoelastic rotating medium with an angular velocity Ω and two temperature at a uniform temperature T_0 , with an initial magnetic field $\mathbf{H}_0 = (0, H_0, 0)$ acting towards y -axis and multi-phase lag heat transfer. The rectangular Cartesian coordinate system (x, y, z) is used. For 2-D problem in xz - plane, we consider

$$\mathbf{u} = (u, 0, w).$$

In addition, we consider that

$$\mathbf{E} = 0, \mathbf{\Omega} = (0, \Omega, 0).$$

From the generalized Ohm's law

$$J_2 = 0. \tag{11}$$

The J_1 and J_3 using (5) are given as

$$J_1 = \frac{\sigma_0 \mu_0 H_0}{1+m^2} \left(m \frac{\partial u}{\partial t} - \frac{\partial w}{\partial t} \right), \tag{12}$$

$$J_3 = \frac{\sigma_0 \mu_0 H_0}{1+m^2} \left(\frac{\partial u}{\partial t} + m \frac{\partial w}{\partial t} \right). \tag{13}$$

Now using the transformation on equations (8)-(9) following Slaughter (2002) are as under

$$\begin{aligned}
c_{11} \frac{\partial^2 u}{\partial x^2} + c_{13} \frac{\partial^2 w}{\partial x \partial z} + c_{44} \left(\frac{\partial^2 u}{\partial z^2} + \frac{\partial^2 w}{\partial x \partial z} \right) - \beta_1 \frac{\partial}{\partial x} \left\{ \varphi - \left(a_1 \frac{\partial^2 \varphi}{\partial x^2} + a_3 \frac{\partial^2 \varphi}{\partial z^2} \right) \right\} \\
- \mu_0 J_3 H_0 = \rho \left(\frac{\partial^2 u}{\partial t^2} - \Omega^2 u + 2\Omega \frac{\partial w}{\partial t} \right),
\end{aligned} \tag{14}$$

$$\begin{aligned}
(c_{13} + c_{44}) \frac{\partial^2 u}{\partial x \partial z} + c_{44} \frac{\partial^2 w}{\partial x^2} + c_{33} \frac{\partial^2 w}{\partial z^2} - \beta_3 \frac{\partial}{\partial z} \left\{ \varphi - \left(a_1 \frac{\partial^2 \varphi}{\partial x^2} + a_3 \frac{\partial^2 \varphi}{\partial z^2} \right) \right\} - \mu_0 J_1 H_0 \\
= \rho \left(\frac{\partial^2 w}{\partial t^2} - \Omega^2 w - 2\Omega \frac{\partial u}{\partial t} \right),
\end{aligned} \tag{15}$$

$$\begin{aligned}
& K_1 \left[1 + \sum_{r=1}^{R_1} \frac{\tau_\theta^r}{r!} \frac{\partial^r}{\partial t^r} \frac{\partial^2 \varphi}{\partial x^2} \right] + K_3 \left[1 + \sum_{r=1}^{R_1} \frac{\tau_\theta^r}{r!} \frac{\partial^r}{\partial t^r} \frac{\partial^2 \varphi}{\partial z^2} \right] \\
& = \left(\varrho + \tau_0 \frac{\partial}{\partial t} + \sum_{r=2}^{R_2} \frac{\tau_q^r}{r!} \frac{\partial^r}{\partial t^r} \right) \left[T_0 \left(\beta_1 \frac{\partial u}{\partial x} + \beta_3 \frac{\partial w}{\partial z} \right) + \rho C_E \left\{ \dot{\varphi} - a_1 \frac{\partial^2 \varphi}{\partial x^2} - a_3 \frac{\partial^2 \varphi}{\partial z^2} \right\} \right]
\end{aligned} \tag{16}$$

and

$$t_{xx} = c_{11}e_{xx} + c_{13}e_{xz} - \beta_1 T, \tag{17}$$

$$t_{zz} = c_{13}e_{xx} + c_{33}e_{zz} - \beta_3 T, \tag{18}$$

$$t_{xz} = 2c_{44}e_{xz}, \tag{19}$$

where

$$\begin{aligned} T &= \varphi - \left(a_1 \frac{\partial^2 \varphi}{\partial x^2} + a_3 \frac{\partial^2 \varphi}{\partial z^2} \right), \\ \beta_1 &= (c_{11} + c_{12})\alpha_1 + c_{13}\alpha_3, \\ \beta_3 &= 2c_{13}\alpha_1 + c_{33}. \end{aligned}$$

To facilitate the solution, below mentioned dimensionless quantities are used

$$\begin{aligned} (x', z') &= \frac{1}{L}(x, z), \quad (u', w') = \frac{\rho c_1^2}{L\beta_1 T_0}(u, w), \quad \Omega' = \frac{L}{c_1}\Omega, \quad a'_1 = \frac{a_1}{L^2}, \quad a'_3 = \frac{a_3}{L^2}, \quad \rho c_1^2 = c_{11}, \\ \varphi' &= \frac{\varphi}{T_0}, \quad (t'_{xx}, t'_{xz}, t'_{zz}) = \frac{1}{\beta_1 T_0}(t_{xx}, t_{xz}, t_{zz}), \quad (\tau'_0, \tau'_\theta, \tau'_q, t') = \frac{c_1}{L}(\tau_0, \tau_\theta, \tau_q, t). \end{aligned} \tag{20}$$

Using (20) in Eqs. (14)-(16) and after suppressing the primes, yield

$$\begin{aligned} \frac{\partial^2 u}{\partial x^2} + \delta_1 \frac{\partial^2 w}{\partial x \partial z} + \delta_2 \frac{\partial^2 u}{\partial z^2} - \frac{\partial}{\partial x} \left\{ \varphi - \left(a_1 \frac{\partial^2 \varphi}{\partial x^2} + a_3 \frac{\partial^2 \varphi}{\partial z^2} \right) \right\} &= \frac{M}{1+m^2} \left[\frac{\partial u}{\partial t} + m \frac{\partial w}{\partial t} \right] + \frac{\partial^2 u}{\partial t^2} \\ &\quad - \Omega^2 u + 2\Omega \frac{\partial w}{\partial t}, \end{aligned} \tag{21}$$

$$\begin{aligned} \delta_1 \frac{\partial^2 u}{\partial x \partial z} + \delta_2 \frac{\partial^2 w}{\partial x^2} + \delta_3 \frac{\partial^2 w}{\partial z^2} - \frac{\beta_3}{\beta_1} \frac{\partial}{\partial z} \left\{ \varphi - \left(a_1 \frac{\partial^2 \varphi}{\partial x^2} + a_3 \frac{\partial^2 \varphi}{\partial z^2} \right) \right\} \\ = -\frac{M}{1+m^2} \left[m \frac{\partial u}{\partial t} - \frac{\partial w}{\partial t} \right] + \frac{\partial^2 w}{\partial t^2} - \Omega^2 w - 2\Omega \frac{\partial u}{\partial t}, \end{aligned} \tag{22}$$

$$\begin{aligned} K_1 \left(1 + \sum_{r=1}^{R_1} \frac{\tau_0^r \partial^r}{r! \partial t^r} \right) \frac{\partial^2 \varphi}{\partial x^2} + K_3 \left(1 + \sum_{r=1}^{R_1} \frac{\tau_0^r \partial^r}{r! \partial t^r} \right) \frac{\partial^2 \varphi}{\partial z^2} \\ = \left(\varrho + \tau_0 \frac{\partial}{\partial t} + \sum_{r=2}^{R_2} \frac{\tau_q^r \partial^r}{r! \partial t^r} \right) \left[\frac{\partial}{\partial t} \left(\delta_6 \frac{\partial u}{\partial x} + \delta_5 \frac{\partial w}{\partial z} \right) + \delta_7 \frac{\partial}{\partial t} \left\{ \varphi - a_1 \frac{\partial^2 \varphi}{\partial x^2} - a_3 \frac{\partial^2 \varphi}{\partial z^2} \right\} \right], \end{aligned} \tag{23}$$

where

$$\delta_1 = \frac{c_{13} + c_{44}}{c_{11}}, \quad \delta_2 = \frac{c_{44}}{c_{11}}, \quad \delta_3 = \frac{c_{33}}{c_{11}}, \quad M = \left(\frac{L\sigma_0 \mu_0^2 H_0^2}{\rho c_1} \right), \quad \delta_6 = \frac{L\beta_1^2 T_0}{\rho c_1}, \quad \delta_5 = \frac{L\beta_1 \beta_3 T_0}{\rho c_1}, \quad \delta_7 = \rho C_E c_1 L.$$

4. Plane wave propagation

We pursue plane wave equations of the form

$$\begin{pmatrix} u \\ w \\ \varphi \end{pmatrix} = \begin{pmatrix} U \\ W \\ \varphi^* \end{pmatrix} e^{i(\omega t - \xi(x \sin\theta - z \cos\theta))}, \tag{24}$$

where $\sin\theta, \cos\theta$ denotes the projection of wave normal to the x - z plane.

Upon using Eq. (24) in Eqs. (21)-(23) we get

$$U[\zeta_1 \xi^2 + \zeta_2] + W[\zeta_3 \xi^2 + \zeta_4] + \varphi^*[\zeta_5 \xi + \zeta_6 \xi^3] = 0, \tag{25}$$

$$U[\zeta_7 \xi^2 + \zeta_8] + W[\zeta_9 \xi^2 + \zeta_{10}] + \varphi^*[\zeta_{11} \xi + \zeta_{12} \xi^3] = 0, \tag{26}$$

$$\zeta_{13} \xi U + \zeta_{14} \xi W + \varphi^*[\zeta_{15} \xi^2 + \zeta_{16}] = 0. \tag{27}$$

and by equating determinant of coefficients of U, W and φ^* to zero we yield the characteristic

equation as

$$A\xi^6 + B\xi^4 + C\xi^2 + D = 0, \quad (28)$$

Where

$$\begin{aligned} A &= \zeta_{13}\zeta_3\zeta_{12} - \zeta_9\zeta_6\zeta_{13} - \zeta_{14}\zeta_1\zeta_{12} + \zeta_7\zeta_6\zeta_{14} + \zeta_9\zeta_1\zeta_{15} - \zeta_{15}\zeta_7\zeta_3, \\ B &= \zeta_3\zeta_{13}\zeta_{11} + \zeta_4\zeta_{12}\zeta_{13} - \zeta_9\zeta_5\zeta_{13} - \zeta_{10}\zeta_6\zeta_{13} - \zeta_{14}\zeta_1\zeta_{11} - \zeta_{14}\zeta_2\zeta_{12} + \zeta_{14}\zeta_7\zeta_5 \\ &\quad + \zeta_6\zeta_8\zeta_{14} + \zeta_{16}\zeta_9\zeta_1 + \zeta_{15}\zeta_9\zeta_2 + \zeta_1\zeta_{10}\zeta_{15} - \zeta_{16}\zeta_3\zeta_7 - \zeta_{15}\zeta_8\zeta_3 - \zeta_{15}\zeta_4\zeta_7, \\ C &= \zeta_{13}\zeta_4\zeta_{11} - \zeta_5\zeta_{10}\zeta_{13} + \zeta_{14}\zeta_8\zeta_5 + \zeta_{16}\zeta_9\zeta_2 + \zeta_{16}\zeta_1\zeta_{10} + \zeta_{10}\zeta_2\zeta_{15} - \zeta_3\zeta_8\zeta_{16} \\ &\quad - \zeta_7\zeta_4\zeta_{16} - \zeta_8\zeta_4\zeta_{15}, \\ D &= \zeta_2\zeta_{10}\zeta_{16} - \zeta_8\zeta_4\zeta_{16} \\ \zeta_1 &= -\sin^2\theta - \delta_2\cos^2\theta, \\ \zeta_2 &= \frac{-M}{1+m^2}i\omega + \omega^2 + \Omega^2, \\ \zeta_3 &= \delta_1\sin\theta\cos\theta, \\ \zeta_4 &= \frac{-Mm}{1+m^2}i\omega - 2\omega\Omega i, \\ \zeta_5 &= i\sin\theta, \\ \zeta_6 &= ia_1\sin^3\theta + ia_3\sin\theta\cos^2\theta, \\ \zeta_7 &= \zeta_3, \\ \zeta_8 &= \frac{Mm}{1+m^2}i\omega + 2\omega\Omega i, \\ \zeta_9 &= \delta_2\sin^2\theta - \delta_3\cos^2\theta, \\ \zeta_{10} &= \frac{-Mm}{1+m^2}i\omega + \omega^2 + \Omega^2, \\ \zeta_{11} &= -i\frac{\beta_3}{\beta_1}\cos\theta, \\ \zeta_{12} &= i\frac{\beta_3}{\beta_1}\cos\theta(a_1\sin^2\theta + a_3\cos^2\theta), \\ \zeta_{13} &= -\left[\varrho + i\omega\tau_0 + \sum_{r=2}^{R_2} \frac{\tau_0^r}{r!}(i\omega)^r\right]\delta_6\omega\sin\theta, \\ \zeta_{14} &= \left[\varrho + i\omega\tau_0 + \sum_{r=2}^{R_2} \frac{\tau_0^r}{r!}(i\omega)^r\right]\delta_5\omega\cos\theta, \\ \zeta_{15} &= -\left[1 + \sum_{r=1}^{R_1} \frac{\tau_0^r}{r!}(i\omega)^r\right][K_1\sin^2\theta + K_3\cos^2\theta] \\ &\quad + \left[\varrho + i\omega\tau_0 + \sum_{r=2}^{R_2} \frac{\tau_0^r}{r!}(i\omega)^r\right]\delta_7i\omega(a_1\sin^2\theta + a_3\cos^2\theta), \\ \zeta_{16} &= \left[\varrho + i\omega\tau_0 + \sum_{r=2}^{R_2} \frac{\tau_0^r}{r!}(i\omega)^r\right]\delta_7i\omega. \end{aligned}$$

The roots of Eq. (25) give six roots of ξ that is, $\pm\xi_1$, $\pm\xi_2$ and $\pm\xi_3$, and we are concerned to the roots with positive imaginary parts. Resultant to these roots, there exists three waves according to descending order of their velocities namely QL, QTS and QT. The phase velocities, attenuation coefficients, specific loss and penetration depth of these waves are obtained by the following expressions.

(i) *Phase velocity*

The phase velocities are given by

$$V_i = \frac{\omega}{\text{Re}(\xi_i)}, i = 1, 2, 3 \quad (29)$$

where V_1, V_2, V_3 are the velocities of QL, QTS and QT waves respectively.

(ii) Attenuation coefficient

The attenuation coefficient is defined as

$$Q_i = \text{Im}g(\xi_i), i = 1, 2, 3. \tag{30}$$

Where Q_1, Q_2, Q_3 are the attenuation coefficients of QL, QTS and QT waves respectively.

(iii) Specific loss

The specific loss is defined as

$$W_i = \left(\frac{\Delta W}{W}\right) i = 4\pi \left| \frac{\text{Im}g(\xi_i)}{\text{Re}(\xi_i)} \right|, i = 1, 2, 3. \tag{31}$$

where W_1, W_2, W_3 are specific loss of QL, QTS and QT waves respectively.

(iv) Penetration depth

The penetration depth of plane wave is given by

$$S_i = \frac{1}{\text{Im}g(\xi_i)}, i = 1, 2, 3. \tag{32}$$

where S_1, S_2, S_3 are penetration depth of QL, QTS and QT waves respectively.

5. Reflection and transmission at the boundary surfaces

We consider a HTI magneto-thermoelastic half-space occupying the region $z \geq 0$. Incident QL, QTS and QT waves at the stress free and thermally insulated surface ($z = 0$) will generate reflected QL, QTS and QT waves in the half-space $z > 0$. The total displacements, conductive temperature

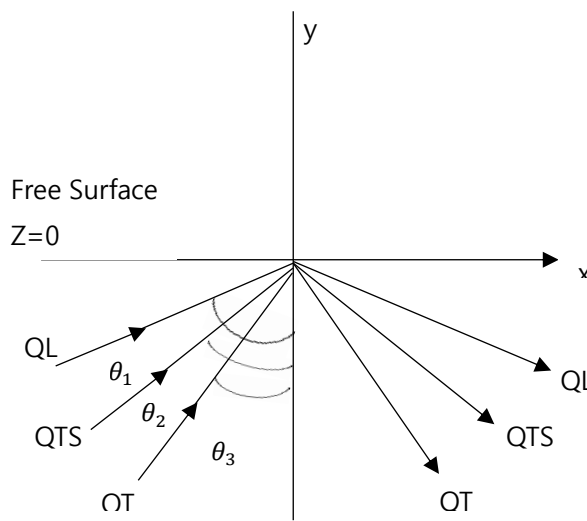


Fig. 1 Geometry of the problem

are given by

$$(u, w, \varphi) = \sum_{j=1}^6 (1, d_j, l_j) B_j e^{iM_j}, \tag{33}$$

where

$$M_j = \omega t - \xi_j(x \sin \theta_j - z \cos \theta_j), j = 1, 2, 3,$$

$$M_j = \omega t - \xi_j(x \sin \theta_j + z \cos \theta_j), j = 4, 5, 6.$$

Here subscripts $j=1, 2, 3$ respectively denote the quantities corresponding to incident QL, QTS and QT-mode, whereas the subscripts $j=4, 5, 6$ denote the corresponding reflected waves, ξ_j are the roots obtained from Eq. (28).

$$d_j = \frac{\zeta_2 \zeta_{16} + (\zeta_2 \zeta_{15j} - \zeta_{5j} \zeta_{13j} + \zeta_{16} \zeta_{1j}) \xi_j^2 + (\zeta_{1j} \zeta_{15j} - \zeta_{6j} \zeta_{13j}) \xi_j^4}{(\zeta_{9j} \zeta_{15j} - \zeta_{12j}) \xi_j^4 + (\zeta_{10} \zeta_{15j} + \zeta_{9j} \zeta_{16} - \zeta_{11j} \zeta_{14j}) \xi_j^2 - \zeta_{10} \zeta_{16}},$$

$$l_j = \frac{(\zeta_2 \zeta_{10} - \zeta_4 \zeta_8) + (\zeta_{10} \zeta_{1j} + \zeta_2 \zeta_{9j} - \zeta_4 \zeta_{7j} + \zeta_8 \zeta_{3j}) \xi_j^2 + (\zeta_{1j} \zeta_{9j} - \zeta_{3j} \zeta_{7j}) \xi_j^4}{(\zeta_{9j} \zeta_{15j} - \zeta_{12j}) \xi_j^4 + (\zeta_{10} \zeta_{15j} + \zeta_{9j} \zeta_{16} - \zeta_{11j} \zeta_{14j}) \xi_j^2 - \zeta_{10} \zeta_{16}}, j=1, 2, 3.$$

$$d_j = \frac{\zeta_2 \zeta_{16} + (\zeta_2 \zeta_{15j} - \zeta_{5j} \zeta_{13j} + \zeta_{16} \zeta_{1j}) \xi_j^2 + (\zeta_{1j} \zeta_{15j} - \zeta_{6j} \zeta_{13j}) \xi_j^4}{(\zeta_{9j} \zeta_{15j} - \zeta_{12j}) \xi_j^4 + (\zeta_{10} \zeta_{15j} + \zeta_{9j} \zeta_{16} - \zeta_{11j} \zeta_{14j}) \xi_j^2 - \zeta_{10} \zeta_{16}}, j=4, 5, 6.$$

$$l_j = \frac{(\zeta_2 \zeta_{10} - \zeta_4 \zeta_8) + (\zeta_{10} \zeta_{1j} + \zeta_2 \zeta_{9j} + \zeta_4 \zeta_{7j} + \zeta_8 \zeta_{3j}) \xi_j^2 + (\zeta_{1j} \zeta_{9j} - \zeta_{3j} \zeta_{7j}) \xi_j^4}{(\zeta_{9j} \zeta_{15j} - \zeta_{12j}) \xi_j^4 + (\zeta_{10} \zeta_{15j} + \zeta_{9j} \zeta_{16} - \zeta_{11j} \zeta_{14j}) \xi_j^2 - \zeta_{10} \zeta_{16}}, j=4, 5, 6.$$

6. Boundary conditions

The dimensionless boundary conditions at the free surface $z=0$, are given by

$$t_{zz} = 0, \tag{34}$$

$$t_{xz} = 0, \tag{35}$$

$$\frac{\partial \varphi}{\partial z} = 0. \tag{36}$$

Using Eq. (33) into the Eqs. (34)-(36), we obtain

$$\sum_{j=1}^3 B_j e^{i(\omega t - \xi_j(x \sin \theta_j))} [-c_{13} i \xi_j \sin \theta_j + c_{33} i d_j \xi_j \cos \theta_j - \beta_3 l_j] - \sum_{j=4}^6 B_j e^{i(\omega t - \xi_j(x \sin \theta_j))} [c_{13} i \xi_j \sin \theta_j + c_{33} i d_j \xi_j \cos \theta_j + \beta_3 l_j] = 0, \tag{37}$$

$$\sum_{j=1}^3 B_j e^{i(\omega t - \xi_j(x \sin \theta_j))} [\xi_j \cos \theta_j - d_j \xi_j \sin \theta_j] - \sum_{j=4}^6 B_j e^{i(\omega t - \xi_j(x \sin \theta_j))} [\xi_j \cos \theta_j + d_j \xi_j \sin \theta_j] = 0, \tag{38}$$

$$\sum_{j=1}^3 B_j e^{i(\omega t - \xi_j(x \sin \theta_j))} [i l_j \xi_j \cos \theta_j] - \sum_{j=4}^6 B_j e^{i(\omega t - \xi_j(x \sin \theta_j))} [i l_j \xi_j \cos \theta_j] = 0. \tag{39}$$

The Eqs. (37)-(39) are satisfied for all values of x , therefore we have

$$M_1(x, 0) = M_2(x, 0) = M_3(x, 0) = M_4(x, 0) = M_5(x, 0) = M_6(x, 0). \tag{40}$$

From Eqs. (33) and (40), we obtain

$$\xi_1 \sin \theta_1 = \xi_2 \sin \theta_2 = \xi_3 \sin \theta_3 = \xi_4 \sin \theta_4 = \xi_5 \sin \theta_5 = \xi_6 \sin \theta_6. \quad (41)$$

The Eqs. (37)-(39) and (41) yield

$$\sum_{p=1}^3 X_{ip} B_p + \sum_{j=4}^6 X_{ij} B_j = 0, \quad (i = 1,2,3), \quad (42)$$

where for $p=1,2,3$ we have

$$X_{1p} = \frac{-c_{13}}{\rho c_1^2} i \xi_p \sin \theta_p + \frac{c_{33}}{\rho c_1^2} i d_p \xi_p \cos \theta_p - \frac{\beta_3}{\beta_1} [1 - a_1 \xi_p^2 \sin^2 \theta_p - a_3 \xi_p^2 \cos^2 \theta_p] l_p, \quad (43)$$

$$X_{2p} = i \xi_p \cos \theta_p - i d_p \xi_p \sin \theta_p, \quad (44)$$

$$X_{3p} = i l_p \xi_p \cos \theta_p. \quad (45)$$

And for $j=4,5,6$ we have

$$X_{1j} = \frac{-c_{13}}{\rho c_1^2} i \xi_j \sin \theta_j - \frac{c_{33}}{\rho c_1^2} i d_j \xi_j \cos \theta_j - \frac{\beta_3}{\beta_1} [1 - a_1 \xi_j^2 \sin^2 \theta_j - a_3 \xi_j^2 \cos^2 \theta_j] l_j, \quad (46)$$

$$X_{2j} = -i \xi_j \cos \theta_j - i d_j \xi_j \sin \theta_j, \quad (47)$$

$$X_{3j} = -i l_j \xi_j \cos \theta_j. \quad (48)$$

AMPLITUDE RATIOS

Incident QL-wave

In case of QL wave, the subscript p takes only one value, that is $p=1$, which means $B_2 = B_3 = 0$. Dividing the set of equations (35) throughout by B_1 , by solving with Cramer's rule we get three homogeneous equations as

$$A_{1i} = \frac{B_{i+3}}{B_1} = \frac{\Delta_i^1}{\Delta}, \quad (49)$$

Incident QTS-wave

In case of QTS wave, the subscript q takes only one value, that is $q=2$, which means $B_1 = B_3 = 0$. Dividing the set of Eq. (35) throughout by B_2 , by solving with Cramer's rule we get three homogeneous equations as

$$A_{2i} = \frac{B_{i+3}}{B_2} = \frac{\Delta_i^2}{\Delta}. \quad (50)$$

Incident QT-wave

In case of QT wave, the subscript q takes only one value, that is $q = 3$, which means $B_2 = B_1 = 0$. Dividing the set of Eq. (35) throughout by B_3 , by solving with Cramer's rule we get three homogeneous equations as

$$A_{3i} = \frac{B_{i+3}}{B_3} = \frac{\Delta_i^3}{\Delta}, \quad (51)$$

Where A_{ji} ($i=1,2,3$) are the amplitude ratios of the reflected QL, QTS, QT-waves to that of the incident QL-(QTS or QT) waves respectively.

Here

$$\Delta = |A_{i(i+3)}|_{3 \times 3}, \quad (52)$$

$$\Delta_i^p, \quad (i = 1, 2, 3). \quad (53)$$

Expression (53) can be obtained by replacing, the 1st, 2nd and 3rd columns of Δ in (52) by $[-X_{1p}, -X_{2p}, -X_{3p}]^T$ respectively.

The energy flux across the surface element is represented as

$$P^* = t_{lm} n_m \dot{u}_l, \quad (54)$$

Where n_m are the direction cosines of the unit normal and \dot{u}_l are the components of the particle velocity.

The time average P^* , is the average energy transmission per unit surface area per unit time and is given at the interface $z=0$ as

$$\langle P^* \rangle = \langle \text{Re}(t_{xz}) \cdot \text{Re}(\dot{u}) + \text{Re}(t_{zz}) \cdot \text{Re}(\dot{w}) \rangle. \quad (55)$$

For complex functions a and b, we take

$$\langle \text{Re}(a) \rangle \langle \text{Re}(b) \rangle = \frac{1}{2} \text{Re}(a\bar{b}). \quad (56)$$

ENERGY RATIOS

The energy ratios $E_i (i=1,2,3)$ expressions for reflected QL, QT, QTH-wave are given as

(i) **QL- wave**

$$E_{1i} = \frac{\langle P_{i+3}^* \rangle}{\langle P_1^* \rangle}, \quad i = 1, 2, 3. \quad (57)$$

(ii) **QTS- wave**

$$E_{1i} = \frac{\langle P_{i+3}^* \rangle}{\langle P_1^* \rangle}, \quad i = 1, 2, 3. \quad (58)$$

(iii) **QT- wave**

$$E_{1i} = \frac{\langle P_{i+3}^* \rangle}{\langle P_1^* \rangle}, \quad i = 1, 2, 3. \quad (59)$$

Where $\langle P_i^* \rangle, i=1, 2, 3$ are corresponding to incident QL, QTS, QT waves respectively and $\langle P_{i+3}^* \rangle, i=1, 2, 3$ are corresponding to reflected QL, QTS, QT waves respectively.

7. Particular cases

i. If $\tau_\theta, \tau_q \rightarrow 0, \tau_0 > 0$ and $q = 1$, in Eqs. (29)-(32), (49)-(51), (57)-(59) we obtain expressions for wave characteristics like phase velocity, specific loss, attenuation coefficients, energy ratios, penetration depths and amplitude ratios of transmitted and reflected waves in a transversely isotropic magneto-thermoelastic solid with two temperature with Lord-Shulman (LS) theory.

- ii. If $\tau_\theta = \tau_q = \tau_0 = 0$ and $\varrho = 1$, in Eqs. (29)-(32), (49)-(51), (57)-(59) we obtain expressions for wave characteristics like phase velocity, specific loss, attenuation coefficients, energy ratios, penetration depths and amplitude ratios of transmitted and reflected waves in a transversely isotropic magneto-thermoelastic solid with two temperature with Coupled Theory of Thermoelasticity (CTE).
- iii. If $\tau_\theta, \tau_q \rightarrow 0, \tau_0 = 1$ and $\varrho = 0$, in Eqs. (29)-(32), (49)-(51), (57)-(59) we obtain expressions for wave characteristics like phase velocity, specific loss, attenuation coefficients, energy ratios, penetration depths and amplitude ratios of transmitted and reflected waves in a transversely isotropic magneto-thermoelastic solid with two temperature with Green-Naghdi-II (GN-II) theory.
- iv. If $\tau_q = \tau_0 > \tau_\theta \geq 0$ and $\varrho = 1, R_1 = R_2 = 1$ and $\tau_q^2 = 0$, in Eqs. (29)-(32), (49)-(51), (57)-(59) we obtain expressions for wave characteristics like phase velocity, specific loss, attenuation coefficients, energy ratios, penetration depths and amplitude ratios of transmitted and reflected waves in a transversely isotropic magneto-thermoelastic solid with two temperature with The simple phase-lags (SPL) theory of Tzou.
- v. If $\tau_0 \rightarrow \tau_q, R_1 = R_2 = 1$ and $\varrho = 1$, in Eqs. (29)-(32), (49)-(51), (57)-(59) we obtain expressions for wave characteristics like phase velocity, specific loss, attenuation coefficients, energy ratios, penetration depths and amplitude ratios of transmitted and reflected waves in a transversely isotropic magneto-thermoelastic solid with two temperature with dual phase-lag theory.
- vi. If $\tau_0 \rightarrow \tau_q, R_1 = 1, R_2 = 2$ and $\varrho = 1$, in Eqs. (29)-(32), (49)-(51), (57)-(59) we obtain expressions for wave characteristics like phase velocity, specific loss, attenuation coefficients, energy ratios, penetration depths and amplitude ratios of transmitted and reflected waves in a transversely isotropic magneto-thermoelastic solid with two temperature with refined multi-dual-phase-lag heat transfer theory and more refinement may be obtained by taking higher values of R_1 and R_2 .
- vii. If we take $c_{11} = c_{33} = \lambda + 2\mu, c_{12} = c_{13} = \lambda, c_{44} = \mu, a_1 = a_3 = a, \beta_1 = \beta_3 = \beta, \alpha_1 = \alpha_3 = a', K_1 = K_3 = K$, in Eqs. (29)-(32), (49)-(51), (57)-(59) we obtain expressions for wave characteristics like phase velocity, specific loss, attenuation coefficients, energy ratios, penetration depths and amplitude ratios of transmitted and reflected waves in an isotropic magneto-thermoelastic solid with two temperature with refined multi-dual-phase-lag heat transfer theory for all above cases(i)-(vi).
- viii. If we take $a_1 = a_3 = 0$ in Eqs. (29)-(32), (49)-(51), (57)-(59) we obtain expressions for wave characteristics like phase velocity, specific loss, attenuation coefficients, energy ratios, penetration depths and amplitude ratios of transmitted and reflected waves in a transversely isotropic magneto-thermoelastic solid without two temperature with refined multi-dual-phase-lag heat transfer theory for all above cases (i)-(vi).

8. Numerical results and discussion

To demonstrate the theoretical results and effect of different theories of thermoelasticity, the physical data for cobalt material, which is transversely isotropic, is taken from Dhaliwal & Singh (1980) as

$$c_{11} = 3.07 \times 10^{11} Nm^{-2}, \quad c_{33} = 3.581 \times 10^{11} Nm^{-2}, \quad c_{13} = 1.027 \times 10^{10} Nm^{-2},$$

$$\begin{aligned}
 c_{44} &= 1.510 \times 10^{11} Nm^{-2}, & \beta_1 &= 7.04 \times 10^6 Nm^{-2}K^{-1}, & \beta_3 &= 6.90 \times 10^6 Nm^{-2}K^{-1}, \\
 \rho &= 8.836 \times 10^3 Kgm^{-3}, & C_E &= 4.27 \times 10^2 jKg^{-1}K^{-1}, & K_1 &= 0.690 \times 10^2 Wm^{-1}K^{-1}, \\
 K_3 &= 0.690 \times 10^2 Wm^{-1}K^{-1}, & K_1^* &= 1.313 \times 10^2 Wsec, & K_3^* &= 1.54 \times 10^2 Wsec, \\
 T_0 &= 298 K, H_0 = 1 Jm^{-1}nb^{-1}, & \mu_0 &= 1.2571 \times 10^{-6} Hm^{-1}, & \epsilon_0 &= 8.838 \times 10^{-12} Fm^{-1}, \\
 L &= 1m, \sigma_0 = 9.36 \times 10^5 col^2 cal^{-1}. cm^{-1} s^{-1}.
 \end{aligned}$$

The values of two Temperature parameters a_1 and a_3 are taken as 0.02, and 0.04 respectively. For the determination of the values of penetration depth, phase velocity, specific loss, attenuation coefficient, amplitude ratios and energy ratios reflected QL, QTS and QT waves w.r.t. incident QL, QTS, and QT waves respectively we have used package MATLAB 8.0.4 and drawn graphically to show the effect of different thermoelastic theories

1. The line in black colour with square symbol represents CTE theory
2. The line in red colour with diamond symbol represents LS theory.
3. The line in blue colour with triangle symbol represent SPL theory.
4. The line in green colour with circle symbol represent RMPL theory.

PHASE VELOCITY

Figs. 2-4 indicate the change of phase velocities w.r.t. frequency ω respectively. The phase velocity V_1 oscillates in the initial range of the frequency for different the theories of thermoelasticity and remain same in rest of the range. In almost all the frequency range and for all the theories of thermoelasticity, the phase velocity V_2, V_3 follows the same pattern.

ATTENUATION COEFFICIENTS

Figs. 5-7 shows that the values of attenuation w.r.t. frequency respectively. From the graphs it is clear that attenuation coefficient Q_1, Q_2 increases for the initial values of the frequencies and then decreases and follows same pattern for all the theories of thermoelasticity. The value of attenuation coefficient Q_3 increases in the initial range of frequency and have same pattern with different magnitude for different theories of thermoelasticity.

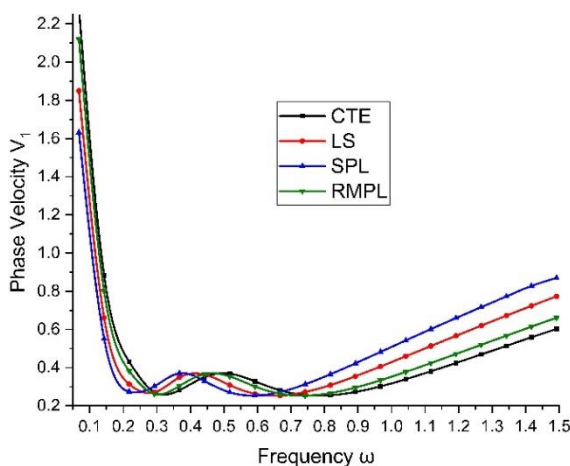


Fig. 2 Variations of phase velocity V_1 with frequency ω

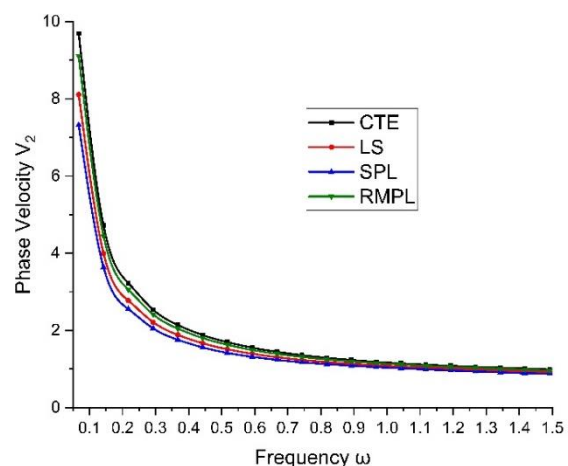


Fig. 3 Variations of phase velocity V_2 with frequency ω

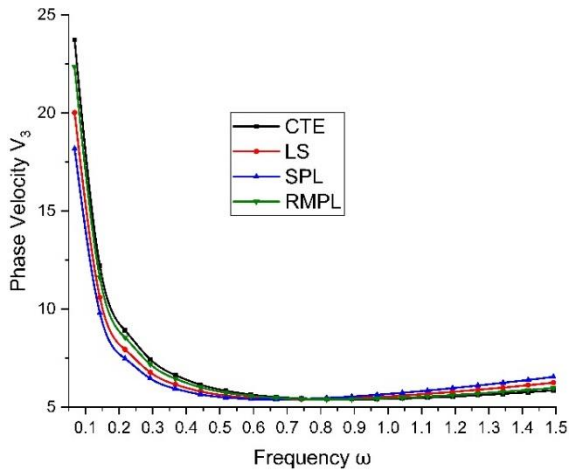


Fig. 4 Variations of phase velocity v_3 with frequency ω

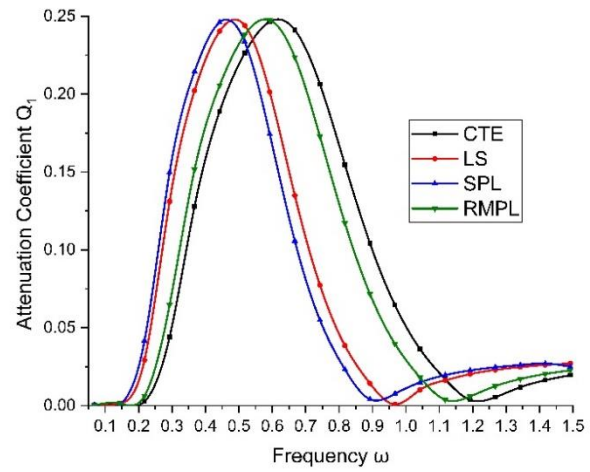


Fig. 5 Variations of attenuation coefficient Q_1 with frequency ω

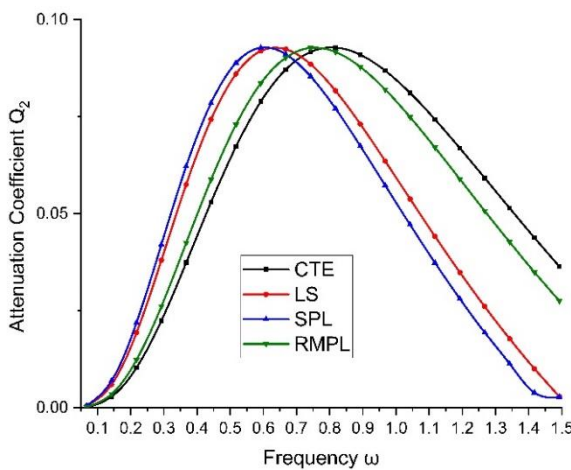


Fig. 6 Variations of attenuation coefficient Q_2 with frequency ω

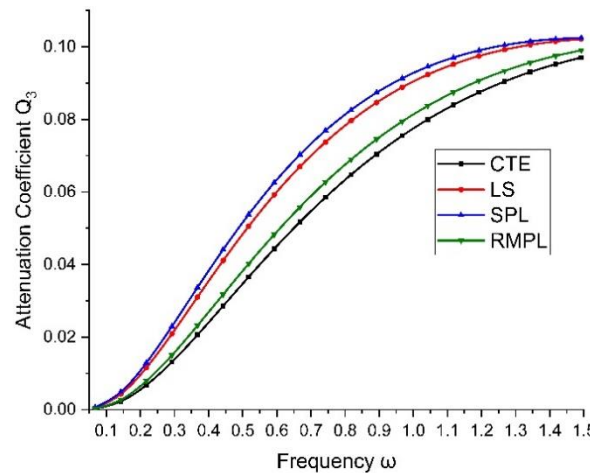


Fig. 7 Variations of attenuation coefficient Q_3 with frequency ω

SPECIFIC LOSS

Figs. 8-10 exhibits the variations of Specific loss w.r.t. frequency. From the graphs it is clear that the value of specific loss W_1 shows the oscillatory pattern for the initial value of the frequency for all the cases and then shows the same magnitude for rest of the range. The value of specific loss W_2 shows increase with the initial value of frequency and then decreases and comes to steady state for rest of the frequency range in all the cases. While the value of specific loss W_3 gradually decreases with different magnitudes for all the theories of thermoelasticity.

PENETRATION DEPTH

Figs. 11-13 shows the variations of penetration depth S_1, S_2, S_3 w.r.t. frequency. Here, we notice a sharp decrease in S_2 and S_3 for all the theories of thermoelasticity and the variations approaches

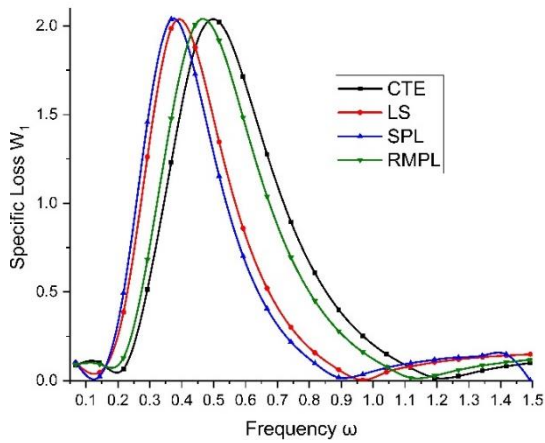


Fig. 8 Variations of specific loss W_1 with frequency ω

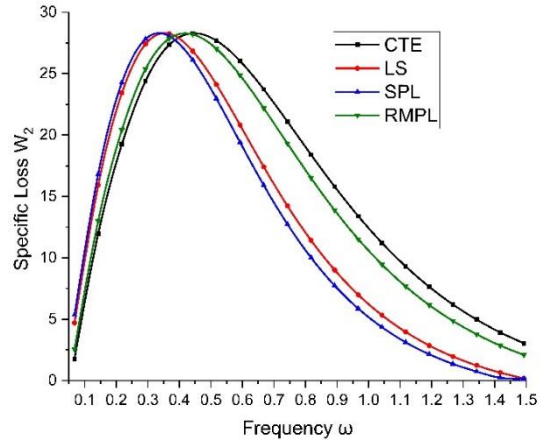


Fig. 9 Variations of specific loss W_2 with frequency ω

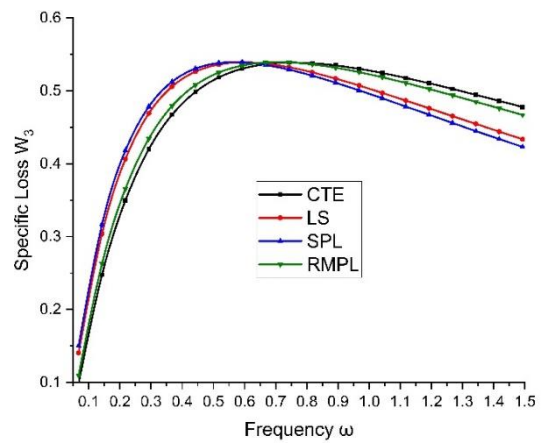


Fig. 10 Variations of specific loss W_3 with frequency ω

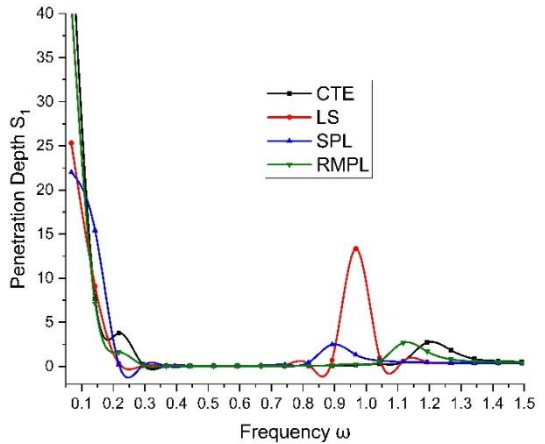


Fig. 11 Variations of penetration depth S_1 with frequency ω

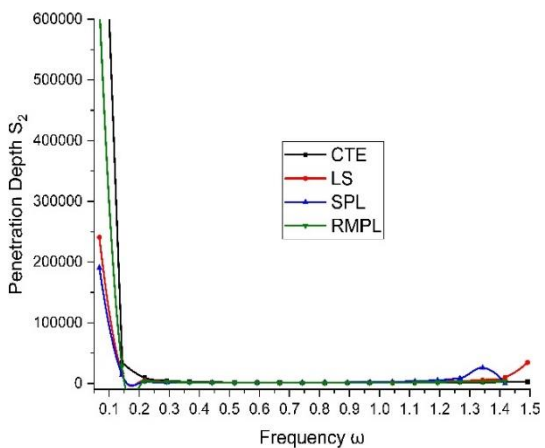


Fig. 12 Variations of penetration depth S_2 with frequency ω

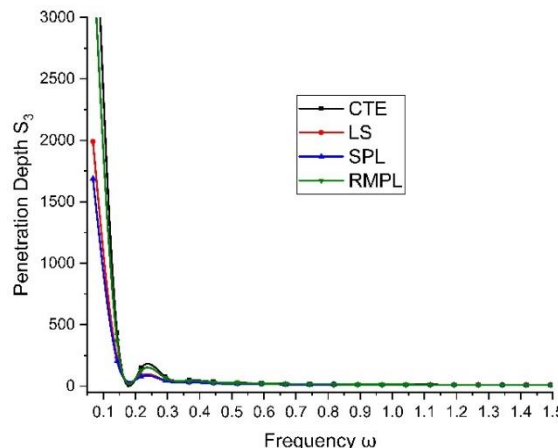


Fig. 13 Variations of Penetration Depth S_3 with frequency ω

to zero for rest of the range of frequency.

ENERGY RATIOS

Incident QL wave

Fig. 14 depicts the change of energy ratio E_{11} w.r.t. angle of incidence θ . It shows that the values of E_{11} increases gradually with the change in angle of incidence corresponding to all the cases of the theories of thermoelasticity. Fig. 15 shows the variations of energy ratio E_{12} w.r.t. angle of incidence θ . Here the value decreases and becomes stationary with a difference in magnitude. Fig. 16 depicts the changes of Energy ratio E_{13} w.r.t. angle of incidence θ . It is noticed that the values increases in the initial range of angle and then remains same for rest of the range angle of incidence θ .

Incident QTS wave

Fig. 17 depicts the change of Energy ratio E_{21} w.r.t. angle of incidence θ . Here corresponding to all the cases, we notice similar increasing trends with difference in magnitudes for the whole range and show significantly variation for different theories of thermoelasticity. Fig. 18 depicts the Variations in E_{22} w.r.t. angle of incidence θ . Here corresponding to all the cases, there is decrease in initial range and then shows steady and similar behavior for rest of range of θ for different theories of thermoelasticity with a small difference in magnitude. Fig. 18. Variations of E_{23} w.r.t. angle of incidence θ are shown in Fig. 19. Here, we notice values increases sharply in the initial range of angle and decrease gradually throughout the range of θ for different theories of thermoelasticity with a small difference in magnitude.

Incident QT wave

Figs. 20-22 depict the Variations of Energy ratios E_{31} , E_{32} , E_{33} w.r.t. angle of incidence θ . Hereafter sharp increase E_{31} , E_{32} and E_{33} , with increase in angle of incidence θ for all the cases of different theories of thermoelasticity with a small difference in magnitude.

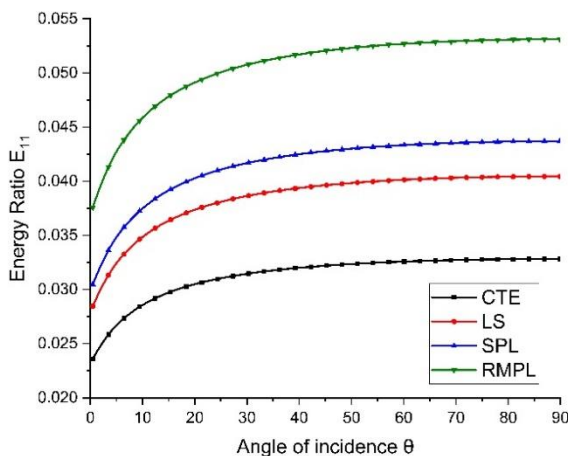


Fig. 14 Variations of energy ratio E_{11} with angle of incidence θ

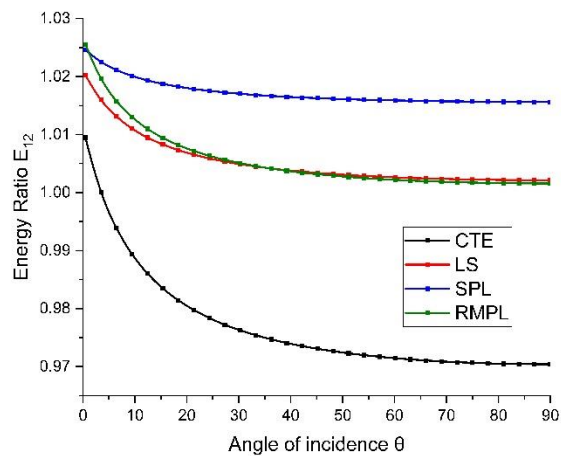


Fig. 15 Variations of energy ratio E_{12} with angle of incidence θ

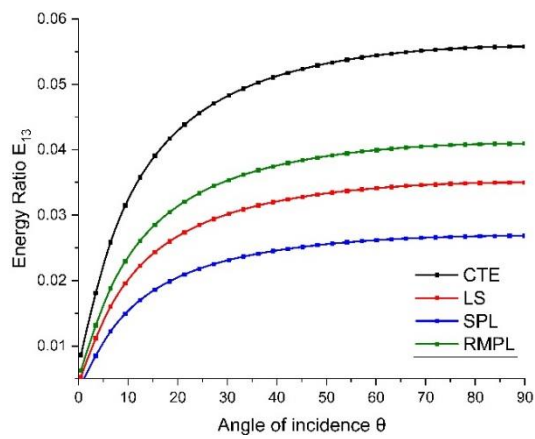


Fig. 16 Variations of energy ratio E_{13} with angle of incidence θ

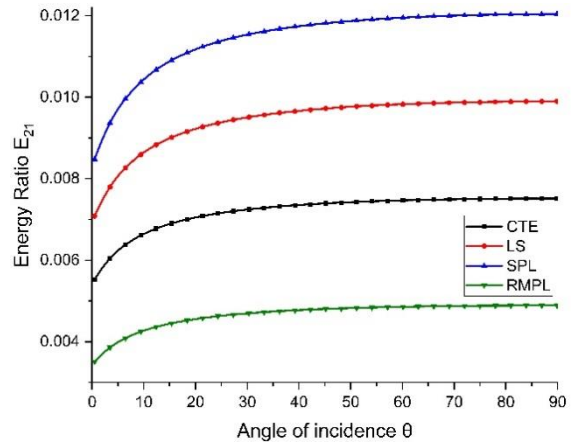


Fig. 17 Variations of energy ratio E_{21} with angle of incidence θ

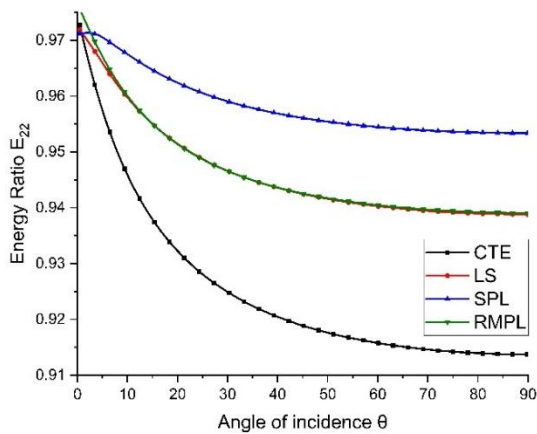


Fig. 18 Variations of energy ratio E_{22} with angle of incidence θ

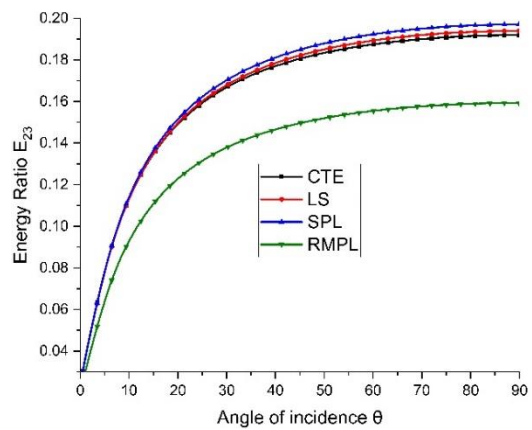


Fig. 19 Variations of energy ratio E_{23} with angle of incidence θ

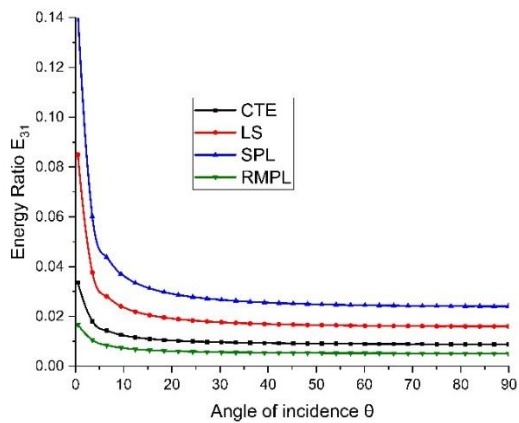


Fig. 20 Variations of energy ratio E_{31} with angle of incidence θ

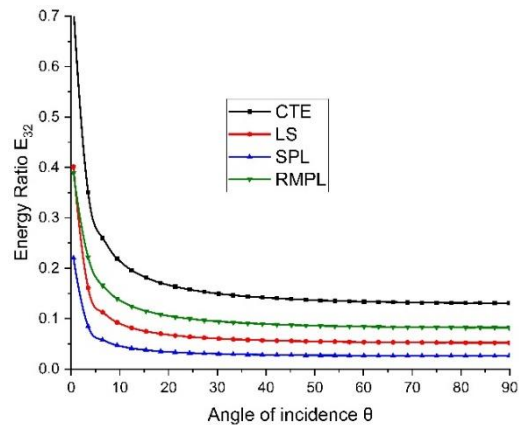


Fig. 21 Variations of energy ratio E_{32} with angle of incidence θ

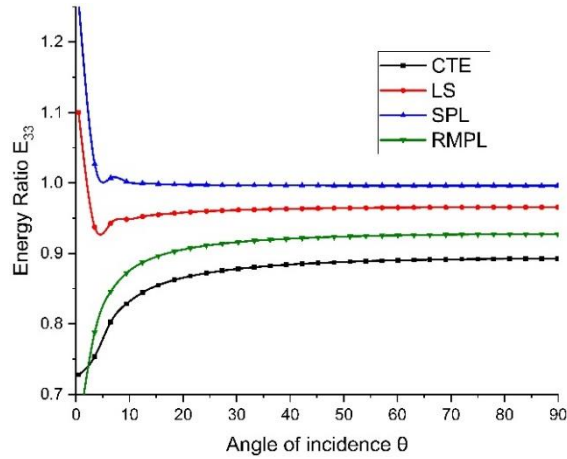


Fig. 22 Variations of energy ratio E_{33} with angle of incidence θ

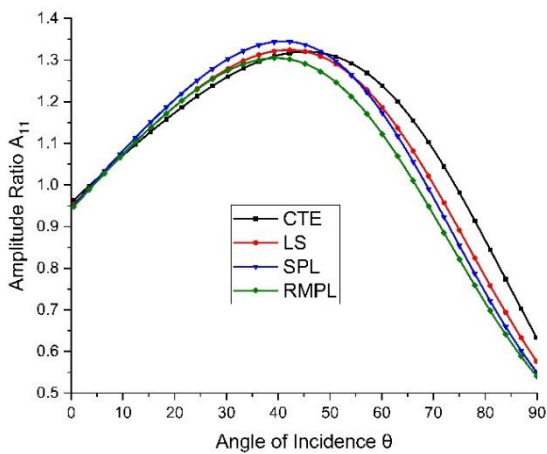


Fig. 23 Variations of amplitude ratio A_{11} with angle of incidence θ

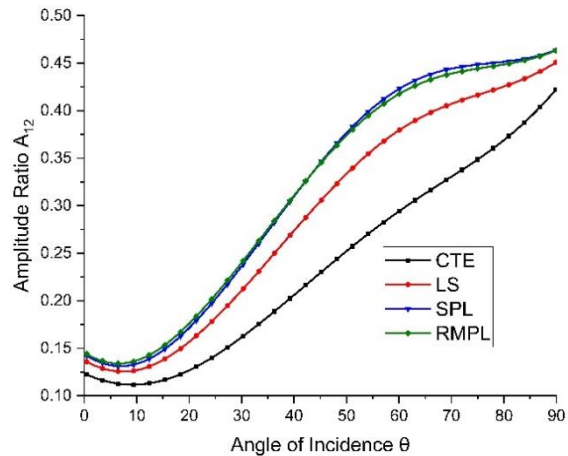


Fig. 24 Variations of amplitude ratio A_{12} with angle of incidence θ

AMPLITUDE RATIOS

Incident QL wave

Figs. 23-25 shows variations of amplitude ratio A_{11} , A_{12} , A_{13} w.r.t. angle of incidence θ . Here, we notice that, initially, there is linear increase in the values of A_{11} for different theories of thermoelasticity with a small difference in magnitude. The amplitude ratio A_{12} and A_{13} shows different pattern with angle of incidence θ for every case of theories of thermoelasticity with a small difference in magnitude.

Incident QTS wave

Figs. 26-28 depicts the variations of amplitude ratio A_{21} , A_{22} , A_{23} w.r.t. angle of incidence θ . Here, we notice that a linear increase in amplitude ratios A_{21} for all the cases of different theories of

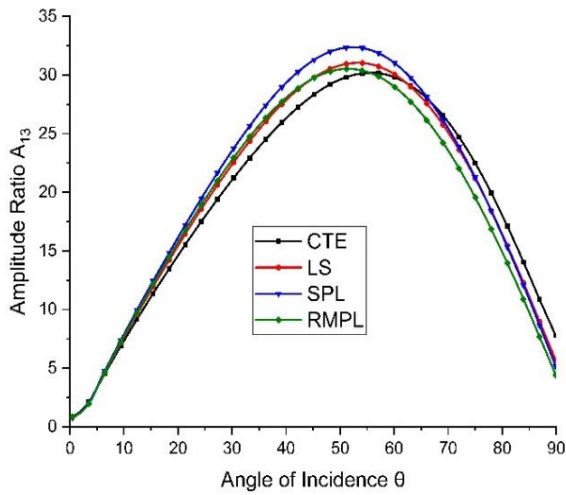


Fig. 25 Variations of amplitude ratio A_{13} with angle of incidence θ

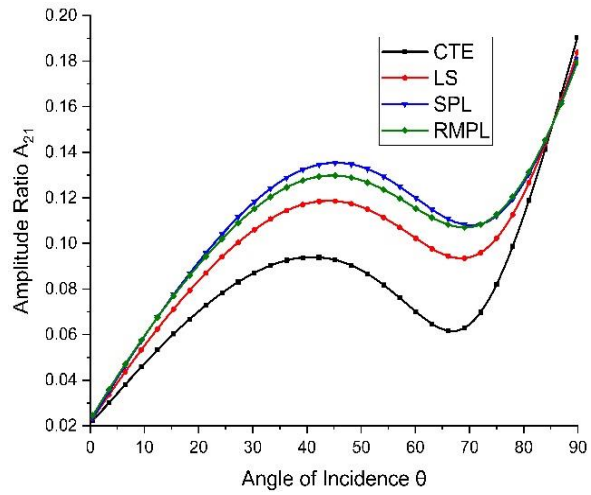


Fig. 26 Variations of amplitude ratio A_{21} with angle of incidence θ

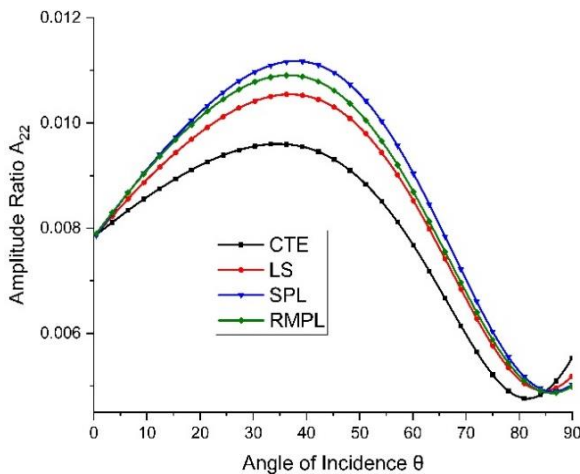


Fig. 27 Variations of amplitude ratio A_{22} with angle of incidence θ

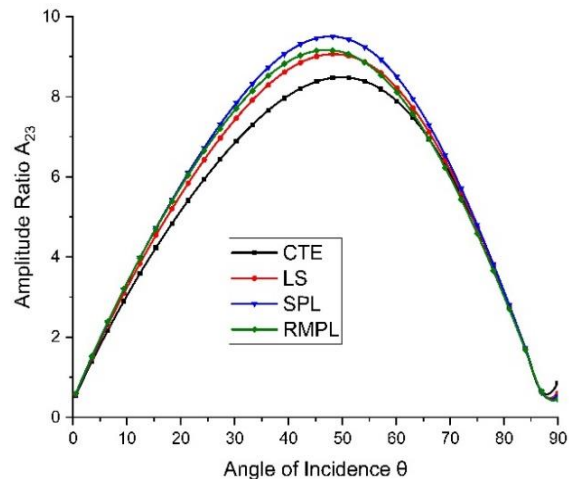


Fig. 28 Variations of amplitude ratio A_{23} with angle of incidence θ

thermoelasticity with a small difference in magnitude while A_{22} and A_{23} shows opposite behaviour for all the cases different theories of thermoelasticity with a small difference in magnitude.

Incident QT wave

Figs. 29-31 show the variations of amplitude ratios A_{31} , A_{32} , A_{33} w.r.t. angle of incidence θ respectively. Here, we notice that there is an increase in the values of amplitude ratios for different theories of thermoelasticity with a small difference in magnitude on the amplitude ratios A_{31} , A_{32} , A_{33} .

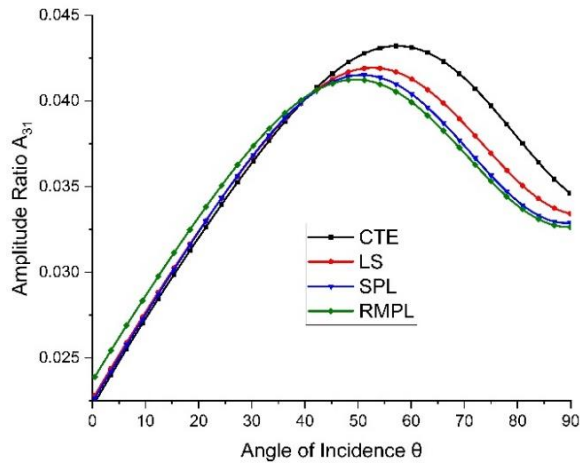


Fig. 29 Variations of amplitude ratio A_{31} with angle of incidence θ

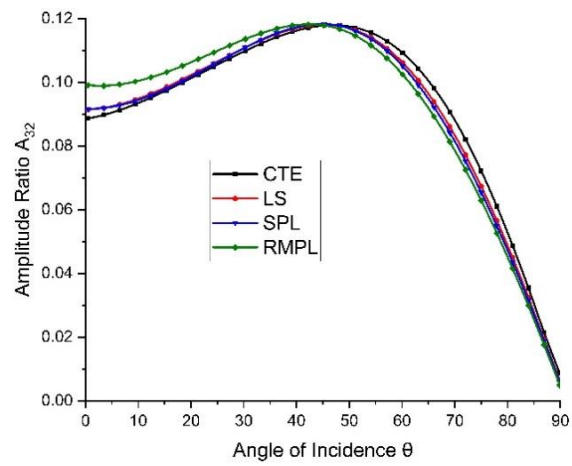


Fig. 30 Variations of amplitude ratio A_{32} with angle of incidence θ

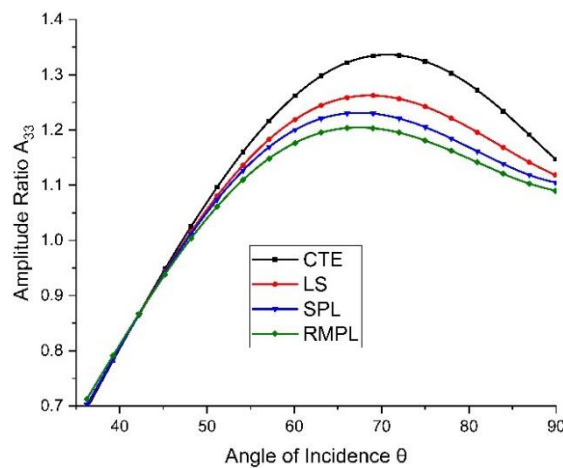


Fig. 31 Variations of amplitude ratio A_{33} with angle of incidence θ

9. Conclusions

- (i) The study exhibits the plane wave propagation in homogeneous transversely isotropic (HTI) magneto-thermoelastic rotating medium with combined effect of Hall current and two temperature due to multi-dual-phase lag heat transfer under different theories of thermoelasticity.
- (ii) The CTE, LS, SPL and RMPL theories of heat transfer have significant effect on the wave characteristics phase velocity, attenuation coefficients, specific loss and penetration depth of various kinds of waves. These theories shows the different behaviors on different wave characteristics.
- (iii) The CTE and RMPL theories of heat transfer have dominating effect on most of the wave characteristics as compared to the LS and SPL theories of heat transfer.
- (iv) The plane wave's signals provides information about the inner earth structure and is also

useful in inspection of materials, magnetometers, geophysics, nuclear fields and related topics.

References

- Abouelregal, A.E. (2013), "Generalized thermoelastic infinite transversely isotropic body with a cylindrical cavity due to moving heat source and harmonically varying heat", *Meccanica*, **48**, 1731-1745. <https://doi.org/10.1007/s11012-013-9705-z>.
- Alesemi, M. (2018), "Plane waves in magneto-thermoelastic anisotropic medium based on (L-S) theory under the effect of Coriolis and centrifugal forces", *International Conference on Materials Engineering and Applications*, 1-12.
- Bhatti, M.M., Elelamy, A.F., Sait, S.M. and Ellahi, R. (2020a), "Hydrodynamics interactions of metachronal waves on particulate-liquid motion through a ciliated annulus: Application of bio-engineering in blood clotting and endoscopy", *Symmetry*, **12**(4), 532-547. <https://doi.org/10.3390/sym12040532>.
- Bhatti, M.M., Ellahi, R., Zeeshan, A., Marin, M. and Ijaz, N. (2019a), "Numerical study of heat transfer and Hall current impact on peristaltic propulsion of particle-fluid suspension with compliant wall properties", *Modern Phys. Lett. B*, **35**(35). <https://doi.org/10.1142/S0217984919504396>.
- Bhatti, M.M., Shahid, A., Abbas, T., Alamri, S.Z. and Ellahi, R. (2020b), "Study of activation energy on the movement of gyrotactic microorganism in a magnetized nanofluids past a porous plate", *Process.*, **8**(3), 328-348. <https://doi.org/10.3390/pr8030328>.
- Bhatti, M.M., Yousif, M.A., Mishra, S.R. and Shahid, A. (2019b), "Simultaneous influence of thermo-diffusion and diffusion-thermo on non-Newtonian hyperbolic tangent magnetised nanofluid with Hall current through a nonlinear stretching surface", *Pramana*, **93**(6), 88. <https://doi.org/10.1007/s12043-019-1850-z>.
- Borejko, P. (1996), "Reflection and transmission coefficients for three dimensional plane waves in elastic media", *Wave Motion*, **24**, 371-393. [https://doi.org/10.1016/S0165-2125\(96\)00026-1](https://doi.org/10.1016/S0165-2125(96)00026-1).
- Chauthale, S. and Khobragade, N.W. (2017), "Thermoelastic response of a thick circular plate due to heat generation and its thermal stresses", *Global J. Pure Appl. Math.*, **13**, 7505-7527.
- Craciun, E.M. and Soós, E. (2006), "Antiplane states in an anisotropic elastic body containing an elliptical hole", *Math. Mech. Solid.*, **11**(5), 459-466. <https://doi.org/10.1177/1081286506044138>.
- Craciun, E.M., Carabineanu, A. and Peride, N. (2008), "Antiplane interface crack in a pre-stressed fiber-reinforced elastic composite", *Comput. Mater. Sci.*, **43**(1), 184-189. <https://doi.org/10.1016/j.commatsci.2007.07.028>.
- Deswal, S. and Kalkal, K.K. (2015), "Three-dimensional half-space problem within the framework of two-temperature thermo-viscoelasticity with three-phase-lag effects", *Appl. Math. Model.*, **39**, 7093-7112. <https://doi.org/10.1016/j.apm.2015.02.045>.
- Dhaliwal, R. and Singh, A. (1980), *Dynamic Coupled Thermoelasticity*, Hindustan Publication Corporation, New Delhi, India.
- Ezzat, M. and Al-Bary, A. (2017), "Fractional magneto-thermoelastic materials with phase lag Green-Naghdi theories", *Steel Compos. Struct.*, **24**(3), 297-307. <https://doi.org/10.12989/scs.2017.24.3.297>.
- Ezzat, M., El-Karamany, A. and El-Bary, A. (2015), "Thermo-viscoelastic materials with fractional relaxation operators", *Appl. Math. Model.*, **39**(23), 7499-7512. <https://doi.org/10.1016/j.apm.2015.03.018>.
- Ezzat, M., El-Karamany, A. and El-Bary, A. (2016), "Generalized thermoelasticity with memory-dependent derivatives involving two temperatures", *Mech. Adv. Mater. Struct.*, **23**(5), 545-553. <https://doi.org/10.1080/15376494.2015.1007189>.
- Ezzat, M.A., El-Karamany, A.S. and Ezzat, S.M. (2012), "Two-temperature theory in magneto-thermoelasticity with fractional order dual-phase-lag heat transfer", *Nucl. Eng. Des.*, **252**, 267-277. <https://doi.org/10.1016/j.nucengdes.2012.06.012>.
- Hassan, M., Marin, M., Ellahi, R. and Alamri, S. (2018), "Exploration of convective heat transfer and flow characteristics synthesis by Cu-Ag/water hybrid-nanofluids", *Heat Transf. Res.*, **49**(18), 1837-1848. doi:10.1615/HeatTransRes.2018025569.
- Kumar, R. and Chawla, V. (2011), "A study of plane wave propagation in anisotropic threephase-lag model and two-phase-lag model", *Int. Commun. Heat Mass Transf.*, **38**, 1262-1268. <https://doi.org/10.1016/j.icheatmasstransfer.2011.07.005>.
- Kumar, R. and Gupta, R.R. (2012), "Plane waves reflection in micropolar transversely isotropic generalized thermoelastic half-space", *Math. Sci.*, **6**(6), 1-10. <https://doi.org/10.1186/2251-7456-6-6>.
- Kumar, R. and Gupta, V. (2015), "Dual-phase-lag model of wave propagation at the Interface between elastic and thermoelastic diffusion media", *J. Eng. Phys. Thermophys.*, **88**(1), 252-265. <https://doi.org/10.1007/s10891-015-1188-4>.

- Kumar, R. and Kansal, T. (2017), "Reflection and refraction of plane harmonic waves at an interface between elastic solid and magneto-thermoelastic diffusion solid with voids", *Comput. Meth. Sci. Technol.*, **23**(1), 43-56.
- Kumar, R., Kaushal, P. and Sharma, R. (2018), "Transversely isotropic Magneto-Visco thermoelastic medium with vacuum and without energy dissipation", *J. Solid Mech.*, **10**(2), 416-434.
- Kumar, R., Sharma, N. and Lata, P. (2016), "Effects of thermal and diffusion phase-lags in a plate with axisymmetric heat supply", *Multidisc. Model. Mater. Struct.*, **12**(2), 275-290. <https://doi.org/10.1108/MMMS-08-2015-0042>.
- Kumar, R., Sharma, N. and Lata, P. (2016), "Thermomechanical interactions in transversely isotropic magnetothermoelastic medium with vacuum and with and without energy dissipation with combined effects of rotation, vacuum and two temperatures", *Appl. Math. Model.*, **40**(13-14), 6560-6575.
- Kumar, R., Sharma, N. and Lata, P. (2017), "Effects of Hall current and two temperatures intrinsically isotropic magnetothermoelastic with and without energy dissipation due to ramp-type heat", *Mech. Adv. Mater. Struct.*, **24**(8), 625-635. <https://doi.org/10.1080/15376494.2016.1196769>.
- Lata, P. and Kaur, I. (2018), "Effect of hall current in transversely isotropic magnetothermoelastic rotating medium with fractional order heat transfer due to normal force", *Adv. Mater. Res.*, **7**(3), 203-220. <https://doi.org/10.12989/amr.2018.7.3.203>.
- Lata, P. and Kaur, I. (2019a), "Transversely isotropic thick plate with two temperature and GN type-III in frequency domain", *Coupl. Syst. Mech.*, **8**(1), 55-70. <https://doi.org/10.12989/csm.2019.8.1.055>.
- Lata, P. and Kaur, I. (2019b), "Study of transversely isotropic thick circular plate due to ring load with two temperature & Green Nagdhi theory of Type-I, II and III", *International Conference on Sustainable Computing in Science, Technology & Management (SUSCOM-2019)*, Amity University Rajasthan, Jaipur, India.
- Lata, P. and Kaur, I. (2019c), "Thermomechanical interactions in transversely isotropic thick circular plate with axisymmetric heat supply", *Struct. Eng. Mech.*, **69**(6), 607-614. <https://doi.org/10.12989/sem.2019.69.6.607>.
- Lata, P. and Kaur, I. (2019d), "Transversely isotropic magneto thermoelastic solid with two temperature and without energy dissipation in generalized thermoelasticity due to inclined load", *SN Appl. Sci.*, **1**, 426. <https://doi.org/10.1007/s42452-019-0438-z>.
- Lata, P. and Kaur, I. (2019e), "Effect of rotation and inclined load on transversely isotropic magneto thermoelastic solid", *Struct. Eng. Mech.*, **70**(2), 245-255. <https://doi.org/10.12989/sem.2019.70.2.245>.
- Lee, G.H., Chung, H.J. and Choi, C.K. (2002), "Adaptive crack propagation analysis with the element-free Galerkin method", *Int. J. Numer. Meth. Eng.*, **56**(3), 331-350. <https://doi.org/10.1002/nme.564>.
- Maitya, N., Barik, S. and Chaudhuri, P. (2017), "Propagation of plane waves in a rotating magneto-thermoelastic fiber-reinforced medium under G-N theory", *Appl. Comput. Mech.*, **11**, 47-58. <https://doi.org/10.24132/acm.2017.328>.
- Marin, M. (1996), "Generalized solutions in elasticity of micropolar bodies with voids", *Revista de la Academia Canaria de Ciencias*, VIII, 101-106.
- Marin, M. (2009), "On the minimum principle for dipolar materials with stretch", *Nonlin. Anal. Real World Appl.*, **10**(3), 1572-1578. <https://doi.org/10.1016/j.nonrwa.2008.02.001>.
- Marin, M. (2010), "A partition of energy in thermoelasticity of microstretch bodies", *Nonlin. Anal. Real World* **11**(4), 2436-2447. <https://doi.org/10.1016/j.nonrwa.2009.07.014>.
- Marin, M. and Nicaise, S. (2016), "Existence and stability results for thermoelastic dipolar bodies with double porosity", *Continuum Mech. Thermodyn.*, **28**(6), 1645-1657. <https://doi.org/10.1007/s00161-016-0503-4>.
- Marin, M., Craciun, E. and Pop, N. (2016), "Considerations on mixed initial-boundary value problems for micropolar porous bodies", *Dyn. Syst. Appl.*, **25**(1-2), 175-196.
- Marin, M., Ellahi, R. and Chirilă, A. (2017), "On solutions of Saint-Venant's problem for elastic dipolar bodies with voids", *Carpath. J. Math.*, **33**(2), 219-232.
- Othman, M.I. and Marin, M. (2017), "Effect of thermal loading due to laser pulse on thermoelastic porous medium under G-N theory", *Result. Phys.*, **7**, 3863-3872. <https://doi.org/10.1016/j.rinp.2017.10.012>.
- Othman, M.I. and Song, Y.Q. (2006), "The effect of rotation on the reflection of magneto-thermoelastic waves under thermoelasticity without energy dissipation", *Acta Mech.*, **184**, 89-204. <https://doi.org/10.1007/s00707-006-0337-4>.
- Othman, M.I. and Song, Y.Q. (2008), "Reflection of magneto-thermoelastic waves from a rotating elastic half-space", *Int. J. Eng. Sci.*, **46**, 459-474. <https://doi.org/10.1016/j.ijengsci.2007.12.004>.
- Othman, M.I., Abo-Dahab, S.M. and S. Alsebaey, O.N. (2017), "Reflection of plane waves from a rotating Magneto-Thermoelastic medium with two-temperature and initial stress under three theories", *Mech. Mech. Eng.*, **21**(2), 217-232.
- Sharma, J.N. and Kaur, R. (2015), "Modeling and analysis of forced vibrations in transversely isotropic thermoelastic thin beams", *Meccanica*, **50**, 189-205. <https://doi.org/10.1007/s11012-014-0063-2>.
- Sinha, S. and Elsibai, K. (1997), "Reflection and refraction of thermoelastic waves at an interface of two semi-infinite media with two relaxation times", *J. Therm. Stress.*, **20**, 129-145. <https://doi.org/10.1080/01495739708956095>.
- Slaughter, W.S. (2002), *The Linearised Theory of Elasticity*, Birkhauser.

- Ting, T.C. (2004), "Surface waves in a rotating anisotropic elastic half-space", *Wave Motion*, **40**, 329-346. <https://doi.org/10.1016/j.wavemoti.2003.10.005>
- Youssef, H.M. (2013), "State-space approach to two-temperature generalized thermoelasticity without energy dissipation of medium subjected to moving heat source", *Appl. Math. Mech., Engl. Edition*, **34**(1), 63-74. <https://doi.org/10.1007/s10483-013-1653-7>.
- Youssef, H.M. (2016), "Theory of generalized thermoelasticity with fractional order strain", *J. Vib. Control*, **22**(18), 3840-3857. <https://doi.org/10.1177/1077546314566837>.
- Zenkour, A. (2018), "Refined microtemperatures multi-phase-lags theory for plane wave propagation in thermoelastic medium", *Result. Phys.*, **11**, 929-937. <https://doi.org/10.1016/j.rinp.2018.10.030>.
- Zhang, L., Arain, M.B., Bhatti, M.M., Zeeshan, A. and Hal-Sulami, H. (2020), "Effects of magnetic Reynolds number on swimming of gyrotactic microorganisms between rotating circular plates filled with nanofluids", *Appl. Math. Mech.*, **41**(4), 637-654. <https://doi.org/10.1007/s10483-020-2599-7>.